# Determining Ruthenium's Optical Constants in the Spectral Range 11-14 nm

L. J. Bissell, D. D. Allred*, R. S. Turley, W. R. Evans, J. E. Johnson
Brigham Young University, Provo UT, 84602

## Abstract

Ruthenium is one material that has been suggested for use in preventing the oxidation of Mo/Si mirrors used in extreme ultraviolet (EUV) lithography. The optical constants of Ru have not been extensively studied in the EUV. We report the complex index of refraction, $1 - \delta + i\beta$, of sputtered Ru thin films from 11-14 nm as measured via reflectance and transmission measurements at the Advanced Light Source at Lawrence Berkley National Laboratory. Constants were extracted from reflectance data using the reflectance vs. incidence angle method and from the transmission data by Lambert's law. We compare the measured indices to previously measured values. Our measured values for $\delta$ are between 14-18% less than those calculated from the atomic scattering factors (ASF) available from the Center for X-ray Optics (CXRO). Our measured values of $\beta$ are between 5-20% greater than the ASF values.

**Keywords:** Ru, multilayers, reflectance, index of refraction, extreme ultraviolet (EUV) lithography, Advanced Light Source

## 1 Introduction

It has been predicted that by 2009, the characteristic dimension (half-pitch) of DRAM features on commercial computer chips will be approximately 45 nm. Projection extreme ultraviolet (EUV) lithography using light with a wavelength of 11-13 nm is a leading technology being developed to meet this need.[1] Molybdenum-containing, particularly molybdenum/silicon, multilayer mirrors will be vital in EUV lithography as they reflect greater than 67% of 13.4 nm light at 5° from normal incidence. However, these mirrors suffer from reflectance losses due to oxidation.[2] Ruthenium is one material that has been suggested for use as a capping layer to prevent the oxidation of Mo/Si mirrors.[2] Ru is a likely candidate since it is the nearest neighbor on the periodic table to molybdenum that does not oxidize under normal conditions. Ru, however, absorbs more light than molybdenum in the spectral range 11-14 nm. The imaginary part of the atomic scattering factor (ASF), f2, for Ru is 2.89 at 13.5 nm, compared to 1.23 for molybdenum.[3]

However, little data has been published on the optical constants of Ru in this spectral range. Windt et al. published data from 2.4-121.6 nm, including data points at 11.4 and 13.5 nm.[4] These are the basis of the ASF Henke et al. reported for Ru at 50 points in the range 0.04-124 nm.[5] These ASF have been extrapolated to include 500 points over a uniform logarithmic mesh and are available from the Center for X-ray Optics (CXRO) website over the same spectral range.[3] We here report our initial determination of the complex index of refraction, $1 - \delta + i\beta$, from our measurements of the reflectance and transmission of sputtered Ru thin films from 11-14 nm.

## 2 Methodology

### 2.1 Depositions and Characterization

Three single-layer Ru samples were prepared in two depositions. Two samples (called A and B) were deposited on silicon substrates for reflectance-as-a-function-of-angle [$R(\theta)$] measurements and one sample (C) was deposited on to an ultrathin membrane for transmission measurements at the same time B was deposited. The silicon substrates used for reflectance measurements were pieces taken from a polished silicon (100 orientation) test wafer. AFM measurements showed the typical rms roughness of similar wafers to be ~0.2 nm over a 100 nm x 100 nm area. Prior to each Ru deposition, the thickness of the native silicon dioxide on each of the silicon substrates was measured using a WVASE 32 spectroscopic ellipsometer from J.A. Woollam Inc. Reflectance sample A was prepared in the first

* allred@byu.edu; phone 1 801 422-3489; fax 1 801 422-0553; http://xuv.byu.edu



Optical Constants of Materials for UV to X-Ray Wavelengths,
edited by Regina Soufli, John F. Seely, Proceedings of SPIE Vol. 5538
(SPIE, Bellingham, WA, 2004) · 0277-786X/04/$15 doi: 10.1117/12.560900

Downloaded From: http://proceedings.spiedigitallibrary.org/ on 03/18/2014 Terms of Use: http://spiedl.org/terms

deposition. In the second deposition, reflectance sample B, and a transmission sample, C, were coated side-by-side on the sample holder. The transmission sample consisted of Ru deposited on an ultrathin (~150nm) polyimide membrane provided to us by MOXTEK, Inc. These membranes are circular; about 1 cm in diameter.

The Ru was deposited via RF magnetron sputtering using a US Inc. Mighty Mak 4-inch gun. We used a Plasmatherm 3KW RF power supply. The incident power was set to 400 W and there was 10 W of reflected power once the plasma lit. The deposition of the Ru films occurred in a high vacuum chamber. The base pressure was less than $1 \times 10^{-4}$ Pa ($8 \times 10^{-7}$ torr), with 1 mT of argon as the working gas pressure.

The deposition system had a crystal monitor positioned to see most of the flux which struck the substrates. This allowed us to achieve the approximate film thickness desired. We obtained a more accurate measurement of each film's thickness using thin film interference. Following each deposition we measured the low-angle (0.6-1.8°) x-ray reflection (XRR) spectrum of the reflectance sample, using a Scintag model XDS 2000 x-ray diffractometer. We measured each sample's low-angle reflectance with Cu-$K_\alpha$ radiation (0.154 nm). To determine the thickness of the Ru layers we compared the observed position of interference minima in the measured XRR spectrum with those modeled for a range of Ru thicknesses on $SiO_2$ on Si substrates. This was accomplished by loading the measured XRR spectrum into IMD.[6] In our IMD model we assumed an rms roughness of 1 nm on the top of the Ru film. The reflectance scale factor was adjusted until the experimental and theoretical curves could be compared on the same log scale. The Ru thickness of the modeled film was varied manually until the width and positions of the peaks of the measured and the modeled data corresponded. The thickness values obtained by this method were used as a constraint on the Ru thickness obtained by modeling EUV reflectance and transmission data.

We did not attempt to measure the thickness of any Ru oxide layers as prior study had showed that the oxidation of Ru under normal conditions is negligible. In the prior study, the deposition of Ru in the same system described above was examined via *in situ* spectroscopic ellipsometry.[7] The Ru sample was exposed to atmospheric air without being removed from the deposition chamber while ellipsometric measurements were made over a 24-hour period. After exposure, there were only slight changes in the ellipsometric $\Delta$ and $\Psi$ data obtained when the sample was in vacuum. The Ru oxide layer thickness was then fit to 0.3 nm using WVASE software.

### 2.2 ALS Reflectometry

Our reflectance and transmission measurements were made at the calibration and standards beamline 6.3.2 at the Advanced Light Source (ALS) at Lawrence Berkeley National Laboratory. An in depth description of beamline 6.3.2 can be found on the CXRO webpage[8] and in Underwood.[9] The beamline provides nearly monochromatic light in the spectral range of approximately 1-25 nm.[10] To determine a sample's reflectance, five parameters must be measured: the signal of the beam reflected from the sample ($S_R$), the signal of the undeflected beam ($S_0$), the background signal (N), the synchrotron beam current at the time of the reflectance measurement (I), and the beam current at the time of the $S_0$ scan ($I_0$). The reflectance is then given by

$$R = \frac{S_R - N}{S_0 - N}\frac{I_0}{I} \qquad (1).$$

#### 2.2.1 Reflectance vs. Incidence Angle Method

For the first reflectance sample, sample A, reflectance as a function of angle, $R(\theta)$, was measured in wavelength steps of 0.5 nm from 11.5 to 14 nm. In a later experiment, $R(\theta)$ of the second sample, sample B, was measured in 0.25 nm steps from 11-14 nm.

Optical constants were then fit to the reflectance data using the reflectance vs. incidence angle method, which has been described by Windt et al.[4] We used JFIT to fit the experimental data to a theoretical model. JFIT is a program which uses the MINUIT algorithm to fit the optical constants and layer thickness(es) of a single layer (or a multilayer) structure to experimental reflectance or transmission data.[11] The current version can also take into account the effects of roughness and non-abrupt interfaces. The version we used, however, did not have the ability to include roughness in the computational model, and no attempt was made to account for roughness in fitting reflectance data.

The reflectance data from samples A and B were fit independently to obtain the film thickness and optical constants. For each sample, an appropriate model of the film was created in JFIT using the measured silicon dioxide and Ru thicknesses as constraints. The optical constants used for the silicon substrate and silicon dioxide layers, as well as the initial constants used for Ru, were taken from the IMD optical constant database. The Ru layer thickness and the layer's complex index of refraction were then determined in a sequential fashion. First the layer's complex index of refraction were then determined using the $R(\theta)$ data at each of seven wavelengths in the range 11-14 nm. Then, these modified constants were then used to obtain a new "best" estimate of the Ru thickness for each of the seven



Downloaded From: http://proceedings.spiedigitallibrary.org/ on 03/18/2014 Terms of Use: http://spiedl.org/terms

wavelengths. The results of each thickness fit were then weighted by their respective errors and, along with the initial XRR thickness value, were summed to obtain a best overall determination of the Ru thickness that was used in subsequent fits. Using this thickness, the complex index of refraction was again fitted at each wavelength and is reported in section 3.

### 2.2.2 Lambert's Law

Lambert's Law provides an independent way to obtain beta. This allows us to check the numbers obtained by reflectance alone. Sample C's transmission was measured at normal incidence from 11.2-13.8 nm in 0.1 nm steps. At each wavelength, we measured the signal of the beam transmitted through the Ru film on the polyimide window ($S_{Ru}$), as well as the signal transmitted through an uncoated polyimide window ($S_{Po}$). $S_0$ and background noise (dark current) scans (N) were also performed. To obtain the transmission, T, through the Ru film, we used:

$$T = \frac{S_{Ru} - N}{S_{Po} - N} \frac{I_{Po}}{I_{Ru}} \quad (2),$$

where $I_{Ru}$ is the synchrotron beam current at the instant of the Ru on polyimide transmission measurement, and $I_{Po}$ is the beam current at the instant of the uncoated polyimide transmission measurement. The absorption coefficient, $\beta$, was extracted from the transmission data using Lambert's Law:[12]

$$T = e^{-4\pi\beta d/\lambda} \quad (3),$$

where d is the measured Ru film thickness and $\lambda$ is the incident wavelength of light. This equation allowed us to obtain a rather accurate value of the Ru film's absorption coefficient without having to measure the polyimide film thickness. The first assumption behind this approach is that the coated and uncoated polyimide windows were the same thickness. Various measurements indicate that the first assumption is substantially correct. The second assumption is that reflection from the various interfaces can be ignored. That is, in order to obtain the correct value of our beta from transmission, we would have to correct for the reflections from the vacuum/Ru, Ru/polyimide, and polyimide/vacuum interfaces for the Ru coated membrane and for the reflections for both polyimide/vacuum interfaces for the uncoated membrane.[12] However, these corrections can be seen to be small and partially cancel at normal incidence in the EUV. In this spectral range, reflectance $\approx$ ¼ ($\delta^2 + \beta^2$). So the total reflectance correction required in calculating $\beta$ from T is less than 0.5% at any wavelength we considered, and was ignored.

## 3 Results and Discussion

### 3.1 Ru Thickness

The initial XRR measurement of sample A at 0.154 nm is displayed in Fig. 1. The discontinuity in the middle of the XRR spectrum corresponds to a time when we increased the current to the x-ray source by a factor of 4 to increase the signal to noise ratio. It can be seen that the measured and calculated peaks in the spectrum do not line up exactly. We found that for sample A, a Ru thickness of 32.1 nm with an uncertainty of 1 nm is the best fit to the XRR data. In the same manner, the Ru thickness of sample B was measured as 21.9 ± 0.5 nm. These uncertainties were used to weight the initial XRR measurements when summing them with the thickness values fit to the reflectance at 11-14 nm.

The results of the Ru thickness measurements, along with the $SiO_2$ thicknesses that were measured with ellipsometry, are shown in Table 1. The thickness of the transmission sample, sample C, was assumed to be the same as sample B.



Downloaded From: http://proceedings.spiedigitallibrary.org/ on 03/18/2014 Terms of Use: http://spiedl.org/terms

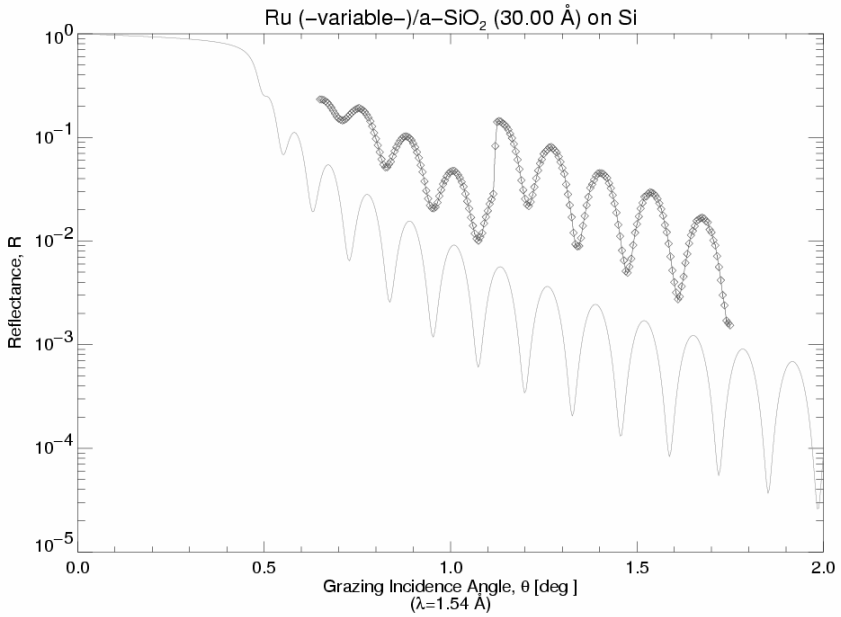



Fig. 1. Using IMD (—) to determine Ru film thickness from XRR data (◊) of the first sample.

Table 1. Film composition of various sputtered Ru thin films. $SiO_2$ thicknesses are shown for the reflectance samples. A—Ru on $SiO_2$ (first deposition). B—Ru on $SiO_2$ (second deposition). C—Ru on polyimide (second deposition)—thickness same as B by assumption.

| Sample | $SiO_2$ thickness (nm) | Ru thickness (nm) |
|---|---|---|
| A | 3.0 | 35.11 |
| B | 3.0 | 21.32 |
| C | - | 21.32 |

The values for the optical constants obtained from fitting the reflectance data are not strongly correlated to the thickness used for the Ru layer in the calculations. The best-fit values for the index of refraction obtained using the Ru thicknesses shown in Table 1 changed inconsequentially from the values obtained using the Ru thickness determined by XRR alone. Specifically, the difference of the real part of the index of refraction, $\delta$, between the fit values was less than 0.1% at any wavelength. In addition, the difference in the imaginary part of the index of refraction, $\beta$, was less than 3% at each wavelength.

### 3.2 Issues relative to fitting reflectance data

Fig. 2 shows a typical fit of the theoretical curve to the experimental reflectance data. The version of JFIT that we used allowed us to enter in a single error value as a percentage for each point in a data set. The error value input into JFIT was the largest signal to noise ratio measured at the ALS for the given data set. For sample A, the reflectance data was assigned an absolute error of 1% at each data point. The data for the sample B was assigned an absolute error of 2%.

We note that there are systematic errors in the reflectance fits. Specifically, for Fig. 2a, there is poor agreement between the theoretical curve with the experimental data past 42°. This feature was noticed in all the reflectance fits for sample A. Another approach to fitting is to use relative error weighting. Relative weighting did better at matching the shape of the experimental data, but the overall agreement between the theoretical and experimental curves was poor so we did not use it.



Downloaded From: http://proceedings.spiedigitallibrary.org/ on 03/18/2014 Terms of Use: http://spiedl.org/terms

Fig. 2b shows a fit of the reflectance data for sample B. Notice that the reflectance minima for the experimental data lie *lower* than the minima in the theoretical curve. We are at a loss on how to account for this fact. Having lower reflectance at minima can occur if the indices of the film are very small or if they are such that the Fresnel coefficients from the top and bottom surfaces are roughly equal, but they cannot be explained by surface roughness or by thickness nonuniformity. Both roughness and thickness nonuniformities would cause the opposite effect, i.e., the minima in the experimental data would not be as low as the theoretical curve that did not account for roughness or the averaging which occurs from nonuniform films.

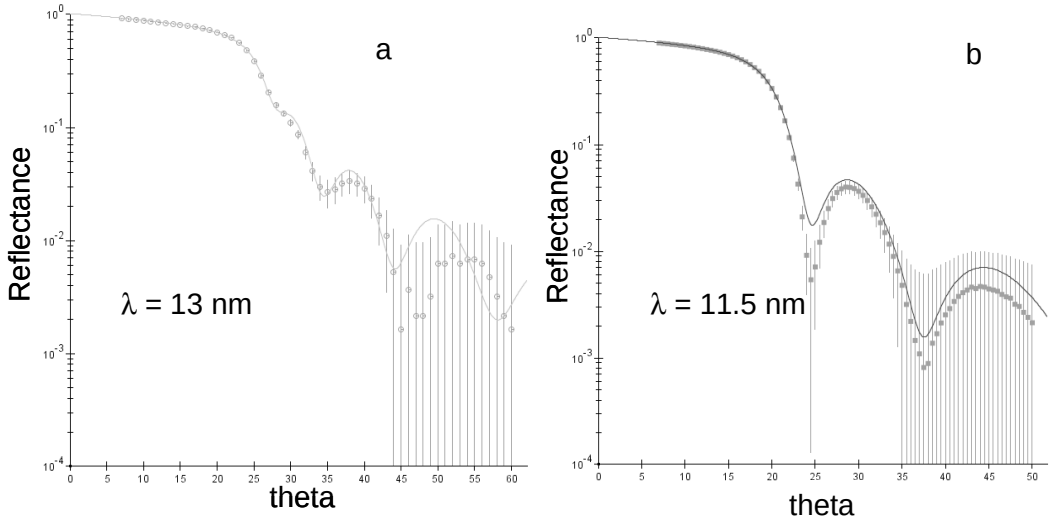



Fig. 2. Typical log plot of the reflectance fits of a) the first sample and b) the second sample. The solid curve is the theoretical reflectance computed by JFIT. The experimental data is shown by the solid shapes. Vertical lines show the attributed error in the reflectance data at each point.

### 3.3 Optical Constants

The best-fit values for δ and β are shown in Figs. 3-6. Also shown for comparison in Figs. 4 and 6 are constants measured by D. L. Windt,[6] by Windt et al.,[4] and as computed from the ASF. These three sets of data were taken from the optical constant database in IMD. IMD specifies the complex index of refraction as n + ik, where $n = 1 - \delta$, and $k = \beta$. The data from Windt is unpublished and comes from measurements made on sputtered Ru films.[6] The values reported by Windt et al. are from reflectance measurements made on Ru films grown by molecular beam epitaxy (MBE).[4] The ASF used to calculate the optical constants in the IMD database were taken from the CXRO webpage.[6] The constants δ and β computed from the ASF are hereafter referred to simply as the *ASF values*.

#### 3.3.1 δ as determined from reflectance R(θ)

Our measurements of δ are shown in Fig. 3-4. The best-fit values obtained from samples A and B are displayed in Fig. 3. The expected error in these values, as given by JFIT, was less than 1%. This error was used to obtain the weighted average of the best-fit value from the two samples together. This weighted average is shown in Fig. 4, with data from the other authors shown for comparison. We note in considering the data in Fig. 3 that the δ best-fit values obtained from the two reflectance samples differ by 17% at 11.5 nm to 24% 14 nm. This is much larger than the error in the determination of δ from R(θ), and we take the interpretation that the difference in δ may be real. The difference between the samples is that B is significantly thinner than A, and may be less dense. In any case, the difference between the data sets increases monotonically with the wavelength. Both data sets follow the same general trend, i.e., δ is an increasing function of the wavelength, as expected.



Downloaded From: http://proceedings.spiedigitallibrary.org/ on 03/18/2014 Terms of Use: http://spiedl.org/terms

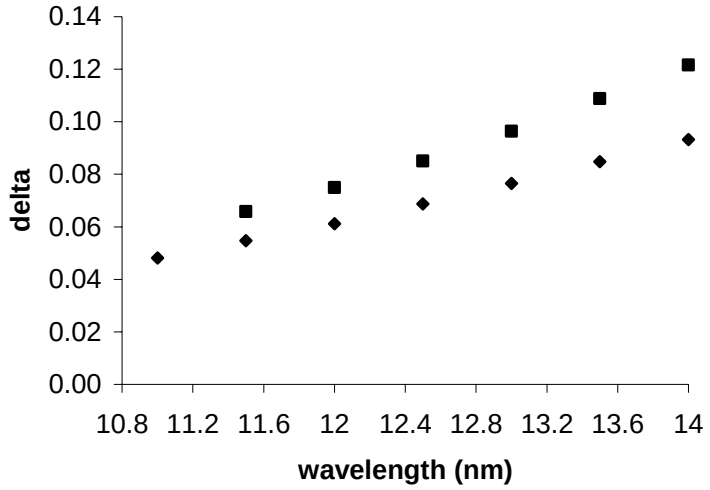



Fig. 3. Best fit values for δ from sample A (■), and sample B (♦).

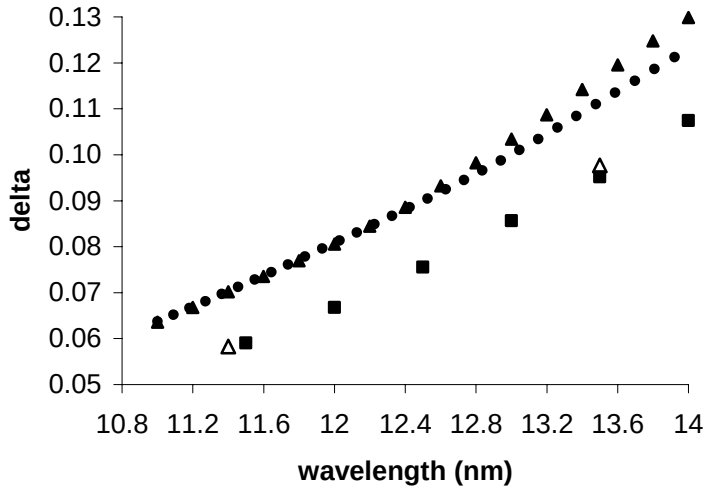



Fig. 4. Ru δ from various sources: this study, weighted average of measured data (■), data from Windt et al.[4] (Δ), the ASF values (●), and unpublished data from D. L. Windt (▲).

In Fig. 4, we see two general trends in the four data sets considered. The unpublished Windt data taken from IMD agrees most closely with the ASF values, while the weighted average value of δ agrees with the data published by Windt et al. In particular, the difference between the ASF value and the weighted average value of δ is 14% at 11.5 nm, and 18% at 14 nm. The weighted average values differ from the unpublished Windt data by a nearly constant value of 18%.

It is interesting to note the difference between the data published by Windt et al. and the δ values that were calculated from these ASF and used in the IMD database (the aforementioned ASF values). We again note that the Windt et al. data was the basis for the ASF used by the CXRO.[5] This discrepancy is likely due to differences in the methods used by Henke et al. in obtaining the ASF from the optical constants published by Windt et al. and the method used by Windt in converting the ASF into the ASF values used in IMD. Finally, we observe that the difference between the ASF values and the Windt et al. data is roughly the same as the difference between our data and the ASF values.



Downloaded From: http://proceedings.spiedigitallibrary.org/ on 03/18/2014 Terms of Use: http://spiedl.org/terms

### 3.3.2 β as determined from reflectance R(θ) and from Lambert's law

β was determined two ways. First, for samples A and B, we used R(θ), as we did with δ. Second, for sample C, we calculated β from transmission data using Lambert's law. To obtain β from the transmission data, we set d = 21.3 nm (sample B's thickness). The error in the absorption coefficient calculated from Lambert's law is 5%. This corresponds to an uncertainty in the thickness measurement of 0.6 nm and a 1% uncertainty in the transmission measurement, due to the signal to noise ratio. The error in the best-fit values given by JFIT was typically 1.5%. For the purpose of comparison, a sixth-order polynomial was fit to the β values calculated from Lambert's law, and a value extrapolated at 14 nm. These three sets of values for β, along with the polynomial fit, are shown in Fig. 5. For clarity, the error bars are not shown. The weighted average of the absorption coefficient from these three measurements is shown in Fig. 6, along with values from the aforementioned sources.

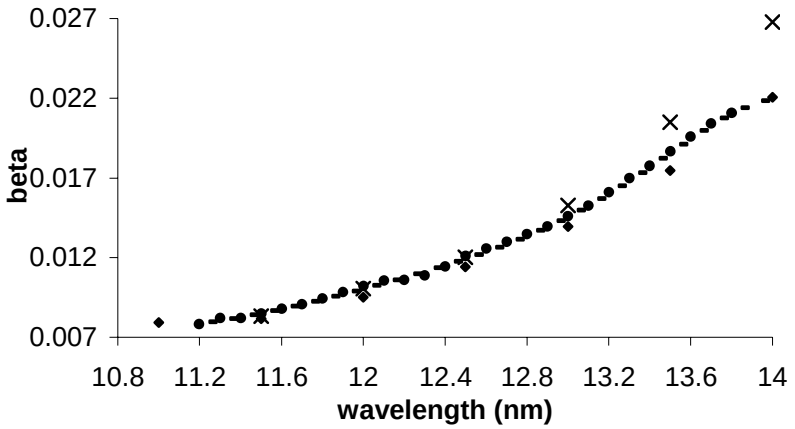



Fig. 5. Best fit values for β from sample A (x), and sample B (♦), values calculated from transmission data for sample C (●), and polynomial fit to data from sample C (-).

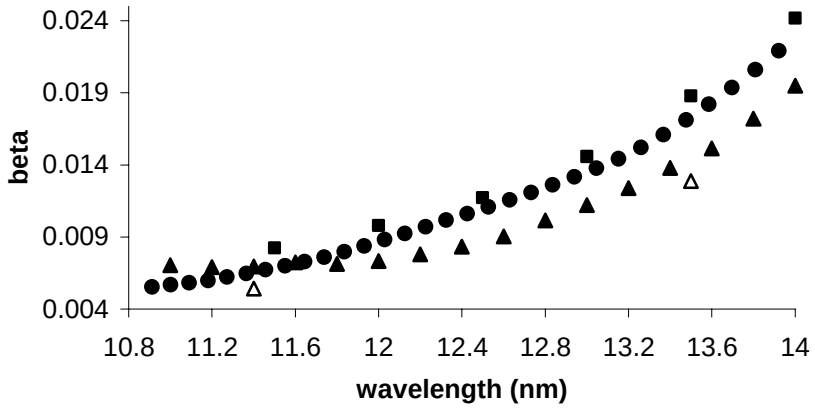



Fig. 6. Weighted average of measured data for β (■), compared with data from Windt et al.[4] (Δ), the ASF values (●), and unpublished data from D. L. Windt (▲).

In Fig. 5, it can be seen that the agreement between the various measured data sets is fairly good for wavelengths less than 13 nm. At 13-14 nm, the values measured from sample A begin to increase with respect to the values measured from samples B and C. Note that for sample C, the data shows steps in the absorption coefficient at 11.4 and 12.2 nm.



Downloaded From: http://proceedings.spiedigitallibrary.org/ on 03/18/2014 Terms of Use: http://spiedl.org/terms

Fig. 6 shows that the shape of weighted average curve is similar to the shape of the ASF curve. The agreement between the two curves is best at 14 nm, where the difference is 6%. At 11.5 nm, the two curves differ by 20%. The shape of the unpublished Windt data is also similar to the ASF values at wavelengths greater than 12.4 nm, where the ASF values are roughly 15% greater than the unpublished Windt data. Below 12.4 nm, the unpublished Windt curve becomes flat. The difference between the Windt et al. data and the ASF values is again apparent. The two curves vary by 18% at 11.4 nm, and by 25% at 13.5 nm.

In summary, we have used the reflectance vs. incidence angle method and Lambert's law to measure the complex index of refraction of Ru over the spectral range 11-14 nm. Comparison with other sources shows differences as great as 20% between our measured $\delta$ and $\beta$ values and those reported by other authors. We will use these results to evaluate the feasibility of a Ru-Mo alloy as a capping layer for Mo/Si multilayer mirrors.

## Acknowledgements

We gratefully acknowledge the support of scholarships from SPIE and BYU, as well as the financial contributions of V. Dean and Alice J. Allred and Marathon Oil Company (US Steel) for gifts to the BYU Department of Physics and Astronomy for thin-film research. We thank Eric Gullikson and Andy Aquila at ALS Beamline 6.3.2 for their help in data interpretation, reduction, and analysis.

## References

[1] also http://public.itrs.net/Files/2003ITRS/Home2003.htm, figure 53, pp. 17-18 of Lithography section. Also D. Atwood, *Soft X-Rays and Extreme Ultraviolet Radiation*, pp. 111-112, (Cambridge, New York, 2000).

[2] S. Bajt, J.B. Alameda, T.W. Barbee Jr., W.M. Clift, J.A. Folta, B. Kaufmann, E.A. Spiller, "Improved reflectance and stability of Mo-Si multilayers," *Opt. Eng.* **41,** 1797-1804 (2002).

[3] http://msxo.lbl.gov/optical_constants/asf.html, June 2003.

[4] D. L. Windt, W. C. Cash, M. Scott, P. Arendt, B. Newman, R. F. Fisher, A. B. Swartzlander, "Optical constants for thin films of Ti, Zr, Nb, Mo, Ru, Rh, Pd, Ag, Hf, Ta, W, Re, Ir, Os, Pt, and Au from 24 Å to 1216 Å," 27 (2), 246-278 (1988).

[5] B.L. Henke, E.M. Gullikson, J.C. Davis. "*X-ray interactions: photoabsorption, scattering, transmission, and reflection at E=50-30000 eV, Z=1-92*," Atomic Data and Nuclear Data Tables, **54** (2), 181-342 (1993).

[6] IMD 4.1.1. Program for EUV and x-ray optics calculations, D.L. Windt. Available at http://cletus.phys.columbia.edu/windt/idl. Optical constant data, along with a description of the source, can be found in the nk directory. The files we used were Ru_llnl_cxro.nk, Ru_windt88.nk, and Ru_windt92.nk.

[7] J. S. Choi, "In situ ellipsometry of surfaces in an ultrahigh vacuum thin film deposition chamber," B.S. dissertation, Department of Physics and Astronomy, Brigham Young University (Provo, UT, 2001).

[8] http://www-cxro.lbl.gov/als6.3.2/, July 2003.

[9] J. H. Underwood, E. M. Gullikson, M. Koike, P. J. Batson, P. E. Denham, K. D. Franck, R. E. Tackaberry, W. F. Steele, "Calibration and standards Beamline 6.3.2 at the Advanced Light Source." Rev. Sci. Instrum., **67** (9), 3372 (1996).

[10] R. L. Sandberg, D. D. Allred, L. J. Bissell, J. E. Johnson, R. S. Turley, "Uranium Oxide as a Highly Reflective Coating from 100-400 eV," in SYNCHROTRON RADIATION INSTRUMENTATION: Eighth International Conference on Synchrotron Radiation Instrumentation, San Francisco, 2003, American Institute of Physics, 796-799 (2004).

[11] Program can be downloaded from http://volta.byu.edu/xray.html. Contact R. S. Turley from the webpage for further questions.

[12] W. R. Hunter, "Measurement of Optical Constants in the Vacuum Ultraviolet Spectral Region," *Handbook of Optical Constants of Solids*, E.D. Palik, pp. 69-87, (Academic, Orlando, 1985).



Downloaded From: http://proceedings.spiedigitallibrary.org/ on 03/18/2014 Terms of Use: http://spiedl.org/terms